Published in final edited form as:
Oncogene. 2014 November 6; 33(45): 5262–5273. doi:10.1038/onc.2013.460.

IGF-1R inhibition enhances radiosensitivity and delays double-strand break repair by both non-homologous end-joining and homologous recombination

Meenali M. Chitnis[1,2], **Kunal A. Lodhia**[1], **Tamara Aleksic**[1], **Shan Gao**[1], **Andrew S. Protheroe**[2], and **Valentine M. Macaulay**[1,2]

[1]Department of Oncology Laboratories, Weatherall Institute of Molecular Medicine, John Radcliffe Hospital, Oxford, OX3 9DS UK

[2]Department of Oncology, Cancer and Haematology Centre, The Churchill Hospital, Old Road, Headington, Oxford, OX3 7LE UK

Abstract

Inhibition of type 1 insulin-like growth factor receptor (IGF-1R) enhances tumor cell sensitivity to ionizing radiation. It is not clear how this effect is mediated, nor whether this approach can be applied effectively in the clinic. We previously showed that IGF-1R depletion delays repair of radiation-induced DNA double-strand breaks (DSBs), unlikely to be explained entirely by reduction in homologous recombination (HR) repair. The current study tested the hypothesis that IGF-1R inhibition induces a repair defect that involves non-homologous end-joining (NHEJ). IGF-1R inhibitor AZ12253801 blocked cell survival and radiosensitized IGF-1R over-expressing murine fibroblasts but not isogenic IGF-1R null cells, supporting specificity for IGF-1R. IGF-1R inhibition enhanced radiosensitivity in DU145, PC3 and 22Rv1 prostate cancer cells, comparable to effects of ATM inhibition. AZ12253801-treated DU145 cells showed delayed resolution of γH2AX foci, apparent within 1hr of irradiation and persisting for 24hr. In contrast, IGF-1R inhibition did not influence radiosensitivity or γH2AX focus resolution in LNCaP-LN3 cells, suggesting that radiosensitization tracks with the ability of IGF-1R to influence DSB repair. To differentiate effects on repair from growth and cell survival responses, we tested AZ12253801 in DU145 cells at sub-SF_{50} concentrations that had no early (≤48hr) effects on cell cycle distribution or apoptosis induction. Irradiated cultures contained abnormal mitoses, and after 5 days IGF-1R inhibited cells showed enhanced radiation-induced polyploidy and nuclear fragmentation, consistent with the consequences of entry into mitosis with incompletely repaired DNA. AZ12253801 radiosensitized DNA-PK proficient but not DNA-PK deficient glioblastoma cells, and did not radiosensitize DNA-PK-inhibited DU145 cells, suggesting that in the context of DSB repair, IGF-1R functions in the same pathway as DNA-PK. Finally, IGF-1R inhibition attenuated repair by both NHEJ and HR in HEK293 reporter assays. These data indicate that IGF-1R

Corresponding author: Dr Valentine Macaulay, Department of Oncology Laboratories, Weatherall Institute of Molecular Medicine, John Radcliffe Hospital, Oxford, OX3 9DS UK. Tel +44(0)1865 222459, Fax 0044(0)1865 222431 valentine.macaulay@oncology.ox.ac.uk.

Conflict of Interest: none declared

Europe PMC Funders Author Manuscripts

influences DSB repair by both major DSB repair pathways, findings that may inform clinical application of this approach.

Keywords

IGF-1R; radiosensitization; DNA repair; double-strand break; non-homologous end-joining; homologous recombination

Europe PMC Funders Author Manuscripts

Introduction

Inhibition or depletion of type 1 insulin-like growth factor receptor (IGF-1R) enhances the sensitivity of human tumor cells to ionizing radiation and cytotoxic drugs (1-4). Consistent with these preclinical data, IGF-1R inhibitory drugs have shown positive effects in Phase I-II trials when combined with chemotherapy (5, 6). However, no such combination has yet proven to be effective in unselected patients in the Phase III setting (7), and there been no reports of the use of IGF-1R inhibitors with radiotherapy. If we can understand how IGF-1R influences the response to DNA damage, it may be possible to use IGF-1R inhibitors more effectively in the clinic.

We previously reported that IGF-1R is up-regulated in primary prostate cancers, and is detectable in prostate cancer metastases (8). Subsequently, other groups have confirmed that prostate cancers over-express IGF-1R (9-12). We showed that IGF-1R depletion enhances the radiosensitivity of prostate cancer cells, and delays repair of DNA double-strand breaks (DSBs; (1, 13). In mammalian cells, DSBs are repaired by non-homologous end-joining (NHEJ) or homologous recombination (HR), a high-fidelity pathway that requires a repair template, typically a sister chromatid, available during late S and G2 phases (14). We recently reported that the DSB repair defect in IGF-1R-depleted prostate cancer cells was accompanied by reduction in repair by HR. This effect may have been related, at least in part, to altered cell cycle distribution in IGF-1R depleted cells, and furthermore, the magnitude of the DSB repair defect suggested that impairment of HR alone was unlikely to explain the repair defect in its entirety (13). The aims of the current study were to determine whether IGF-1R inhibition induces a similar delay in DSB repair, and if so, to quantify repair via the major DSB repair pathways. We find that IGF-1R inhibition induces radiosensitization that is associated with attenuation of both NHEJ and HR, and with induction of polyploidy and late nuclear fragmentation, a phenotype that is consistent with entry into mitosis with incompletely repaired DNA.

Results

IGF-1R inhibition radiosensitizes IGF-1R over-expressing murine fibroblasts but not IGF-1R null cells

We investigated effects of IGF-1R inhibition using AZ12253801, an IGF-1R tyrosine kinase inhibitor that shows ~10-fold selectivity over the insulin receptor (15, 16). Initially, to determine whether AZ12253801 exerts its effects predominantly via IGF-1R, we used IGF-1R–null murine fibroblasts (R− cells) and isogenic R+ cells over-expressing human

IGF-1R (Figure 1a; (17). In R+ cells, AZ12253801 blocked IGF-induced IGF-1R phosphorylation (Figure 1b) and inhibited cell survival with SF_{50} (concentration that inhibits survival to 50%) of 80nM (Figure 1c, Supplementary Figure S1). In contrast, IGF-1R null R − cells showed negligible response to AZ12253801, and the SF_{50} was not achieved (Figure 1c). The differential effect of AZ12253801 in R+ and R− cells supports the contention that the major mechanism of action of AZ12253801 is via IGF-1R inhibition. R+ cells were significantly more radioresistant than R− cells, as previously reported (18), and were radiosensitized by AZ12253801. In contrast, AZ12253801 did not influence radiosensitivity of IGF-1R null R− cells (Figure 1d). It was noted that IGF-1R inhibition suppressed post-irradiation survival of R+ cells to the level in R− cells, suggesting that IGF-1R expression is the principal factor contributing to radioresistance in R+ cells.

Prostate cancer cells are radiosensitized by IGF-1R-inhibition and show features of mitotic catastrophe and delayed nuclear fragmentation after radiation

Next, we tested effects of AZ12253801 on radiosensitivity in prostate cancer cells, following initial characterization of IGF axis components (Figure 2a). Assessment of intrinsic radiosensitivity indicated that DU145 cells were the most radioresistant, PC3 and LNCaP-LN3 intermediate, and 22Rv1 more radiosensitive (Figure 2b). In DU145 cells, AZ12253801 caused dose-dependent inhibition of IGF-1R phosphorylation that persisted for ~48hr, suppressed activation of AKT and ERKs, and inhibited cell survival with SF_{50} 60nM (Figure 2c-e). To address concerns that IGF-1R inhibition may not persist for the duration of clonogenic assays, potentially underestimating the phenotype, these assays were repeated, replacing AZ12253801 every 2 days. However, this did not increase inhibitory effects on cell survival (not shown). We also determined AZ12253801 SF_{50} values in PC3, 22Rv1 and LNCaP-LN3 cells (Table 1). In contrast to findings in isogenic R+/R− cells, there was no correlation between radiosensitivity and IGF-1R expression or SF_{50} for IGF-1R inhibition, likely because of genotypic differences between the prostate cancer cell lines (Table 1, Figure 2a).

Radiation survival assays were performed to test effects of AZ12253801, applied at or below the SF_{50} concentration for each cell line, and comparing with radiosensitization induced by ATM inhibitor KU55933. At 30-60nM, AZ12253801 caused dose-dependent radiosensitization of DU145 cells (Figure 2f). Indeed, effects of 60nM AZ12253801 were comparable to radiosensitization induced by KU55933, supporting the contention that IGF-1R inhibition has a biologically significant effect on radiation sensitivity. Assessment of parallel DU145 cultures following *IGF1R* gene silencing (Figure 2g) indicated that IGF-1R depletion and inhibition induced equivalent radiosensitization. AZ12253801 also enhanced radiosensitivity of PC3 and 22Rv1 cells, and as in DU145, this effect was comparable to radiosensitization induced by ATM inhibition (Table 1, Supplementary Figure S2a, b). In contrast, LNCaP-LN3 cells showed no major change in radiosensitivity when IGF-1R was inhibited, and neither were they radiosensitized by ATM inhibitor KU55933 (Supplementary Figure 2c). We previously noted that IGF-1R depletion did not radiosensitize LNCaP cells (13), speculating that this could relate to very low IGF-1R expression or absence of the IGF-1R adaptor protein insulin receptor substrate-1 (IRS-1, Figure 2a; (19). However, LNCaP-LN3 was not the most radiosensitive of the cell lines we

tested (Figure 2b), suggesting that other factors may over-ride effects of low IGF-1R. Indeed, LNCaP-LN3 cells were isolated from sequential lymph node metastases, and are known to express high levels of anti-apoptotic (Bcl2) and low levels of pro-apoptotic (BAX, BAK) proteins and to be resistant to apoptosis (20). These cells also express mutant PTEN, and we noted that IGF-1R inhibitor NVP-AEW541 was reported not to radiosensitize PTEN null PC3 cells (3). However, we find that AZ12253801 induced comparable radiosensitization in PC3 and DU145 cells, similar to effects of *IGF1R* gene silencing (13), suggesting that lack of functional PTEN does not necessarily render cells refractory to the radiosensitizing effects of IGF-1R inhibition. Collectively, these experiments support a role for IGF-1R in mediating post-irradiation survival in 3 of 4 human prostate cancer cell lines, and in murine fibroblasts that express IGF-1R.

IGF-1R has well-established roles in regulating cell cycle progression and apoptosis, properties that influence cell survival after irradiation (21, 22). We investigated whether IGF-1R inhibition has any influence on the radiation response that is independent of these well-characterized roles, and employed several strategies to limit cell cycle and apoptotic responses to IGF-1R inhibition. Firstly, we performed experiments in DU145 cells, which harbor mutant p53 and non-functional Rb (http://cancer.sanger.ac.uk; (23), and in which we previously demonstrated a DSB repair defect upon IGF-1R depletion (13). Secondly, we used AZ12253801 at sub-GI_{50} concentrations to limit confounding effects on proliferation and cell survival. The GI_{50} value for AZ12253801 is 120nM in DU145 cells (15), and so subsequent experiments used AZ12253801 at 30-60 nM, as in R+ and R− cells.

IGFs promote transition from G1 to S and G2 to M phases of the cell cycle via up-regulation of cyclins, enhancement of cyclin-dependent kinase (CDK) activity and retinoblastoma (Rb) protein phosphorylation, and IGF-1R inhibition induces cell cycle arrest in G1 or G2 (22, 24-27). This is relevant because intrinsic radiosensitivity varies during the cell cycle, and the ability to utilize HR depends on cell-cycle dependent availability of a homologous template (14, 28, 29). However, in p53 mutant, Rb null DU145 cells, 30nM AZ12253801 did not influence cell cycle profiles in undamaged cells (Supplementary Table 1, upper; Supplementary Figure S3a). Control-treated cells showed G2-M arrest 6-8hr after 3Gy, and this was not altered at time-points up to 48hr post-irradiation by 30nM AZ12253801 (Supplementary Table 1, lower; Supplementary Figure S3a). Apoptosis assays revealed apoptosis induction in cells that were AZ12253801-treated or irradiated, although the addition of 30-60nM AZ12253801 did not further enhance irradiation-induced apoptosis at 24-48hr (Supplementary Figure 3b). These data suggest that early (≤48hr) apoptosis induction or changes in cell cycle distribution are unlikely to make a major contribution to radiosensitization induced by AZ12253801. Similar lack of apoptosis enhancement was observed in colorectal cancer cells treated with IGF-1R inhibitor PQIP together with SN38, the active metabolite of irinotecan (26).

Having found no significant differences in early (≤48hr) changes in cell cycle distribution or apoptosis induction, we next tested whether AZ12253801 was capable of inducing relatively late changes that could influence cell viability following irradiation. Senescence is known to inhibit access of repair factors to DSBs via increase in heterochromatin, and there are conflicting data on the contribution of the IGF axis to senescence induction (30-34).

However, we found no evidence that AZ12253801-induced senescence in irradiated DU145 cells (Supplementary Figure 3c), perhaps related to the absence of functional Rb or p16 in these cells (35). Finally, radiation is known to induce mitotic catastrophe, characterized by atypical mitoses, leading after one or more rounds of replication to appearance of polyploid cells that may subsequently die by apoptosis (36, 37). This is distinct from apoptosis induced soon after irradiation, which was not enhanced by IGF-1R inhibition (Supplementary Figure 3b). Therefore, we co-stained irradiated DU145 cells for phospho-histone H3 and β-tubulin to assess mitotic fraction and spindle morphology respectively. Undamaged control or AZ12253801-treated cells contained normal spindles with correct chromosome segregation (Figure 3a). One day after irradiation, we detected abnormal mitoses in both control and IGF-1R inhibited cultures, with evidence of lagging DNA strands, aberrant spindles, and micronucleus formation. By 5 days many cells had died, particularly following AZ12253801 treatment, and both cultures contained large cells with large abnormal fragmented nuclei (Figure 3a). In order to quantify differences between control and AZ12253801-treated cells, we performed flow cytometric analysis of mitotic index (phospho-histone H3 positivity) and DNA content (Figure 3b, Table 2). IGF-1R inhibition did not appear to induce a detectable increase in mitotic index (Table), but there was increased polyploidy (>4N DNA content) 5 days after 10Gy irradiation, and a large increase in nuclear fragmentation as quantified by sub-G1 fraction (Table). These data are consistent with late triggering of apoptosis following several rounds of aberrant mitosis, which can result from incompletely or aberrantly repaired DNA (37).

IGF-1R inhibition delays resolution of radiation-induced γH2AX

Ionizing radiation causes a variety of DNA lesions of which DSBs are the most toxic (14). We and others have shown that IGF-1R regulates components of the cellular response to DNA damage, with evidence for altered repair of radiation-induced DSBs in IGF-1R-depleted cells (1, 13, 38, 39). To investigate whether similar changes occur upon IGF-1R inhibition, we assessed DSB induction and repair by quantifying γH2AX, the phosphorylated form of the variant histone H2AX (40). Initial assessment by western blot indicated that irradiated control-treated DU145 cells showed resolution of γH2AX to basal (unirradiated) levels by 24hrs, while pre-treatment with 30nM AZ12253801 induced a delay in the resolution of γH2AX signal that was apparent at 4 hours ($p<0.01$), with a similar trend persisting 24-48hr post-irradiation (Figure 4a, b). Although our data indicated that 30nM AZ12253801 did not appear to influence early (≤48hr) radiation-induced changes in cell cycle distribution or apoptosis (Supplementary Table S2, Supplementary Figure S3b), we were mindful that γH2AX can be induced during S-phase and by apoptosis, in the latter case typically forming a ring around the nuclear periphery, progressing to widespread diffuse signal (41-43). Therefore, we also assessed γH2AX by immunofluorescence. Intense pan-nuclear γH2AX was detected in a minority of cells 24-48 hour post-irradiation, both in control and AZ12253801-treated cells (Figure 4c). These appearances were consistent with features of apoptosis; such cells were excluded from subsequent analysis, which quantified only discrete focal γH2AX. After quantifying γH2AX foci in DU145 cells following 1-10Gy irradiation, we selected 3Gy as a dose at which foci were induced in the linear range, and could be accurately counted (Supplementary Figure S4a). These foci could be co-stained for 53BP1, which form rapidly at the site of DNA DSBs (44), confirming that focal γH2AX

represented DSBs (Supplementary Figure S4b). Unirradiated cells contained few γH2AX foci (mean 2.6 ± 0.3 foci per cell in controls, 2.4 ± 0.4 in IGF-1R inhibited cells; Figure 4d), with significant increase 1hr after irradiation, resolving in control-treated cells to basal levels at 24hr. In cells pre-treated with 30nM AZ12253801, there was a modest but significant excess of γH2AX foci 1hr following irradiation, with a delay in resolution that persisted for 24hr (Figure 4e). These results were comparable with the DSB repair delay that we detected previously in IGF-1R depleted cells by quantification of γH2AX foci and pulsed field gel electrophoresis (13). To determine whether the increase in focus formation at 1hr was due to increased induction or delayed resolution of damage, foci were quantified at earlier time points. Maximal damage was apparent by 30min, with no difference between controls and AZ12253801-treated cells, and with a subsequent delay in focus resolution from 1hr post-irradiation (Figure 4f). These data are consistent with a DNA repair delay, evident from early time-points after DNA damage, in IGF-1R inhibited cells.

Given that LNCaP-LN3 cells had not been radiosensitized by IGF-1R inhibition (Supplementary Figure S2c) we also tested whether AZ1253801 influenced γH2AX focus formation in these cells. In control-treated LNCaP-LN3 cells, focus induction and resolution followed a time-course similar to that seen in control DU145 cells, and it was clear that IGF-1R inhibition made no difference to this pattern (Supplementary Figure S4c). This suggests that the ability of IGF-1R inhibition to enhance radiosensitivity tracks with its ability to influence γH2AX focus resolution, supporting the concept that IGF-1R makes an important contribution to radio-resistance via its impact on DSB repair.

IGF-1R inhibition attenuates repair by NHEJ

We next investigated the molecular basis for delayed DSB repair. Previous study of murine melanoma cells showed that IGF-1R depletion enhanced radiosensitivity and impaired ATM kinase activity (45). In human MCF7 breast cancer cells binding is detectable between ATM and IRS-1 (46). However, in DU145 cells, where IRS-1 is almost exclusively cytoplasmic (13), we could not detect interaction between ATM and IGF-1R or IRS-1 (Supplementary Figure S5a), and there was no evidence of a functional ATM defect in IGF-1R-inhibited cells (Supplementary Figure S5b). In murine fibroblasts that express human IGF-1R, IRS-1 is reported to interact with the recombinase RAD51, influencing its ability to form damage-induced foci and to contribute to HR (38). In previous work we were unable to detect IRS-1:RAD51 complexes, but did detect reduction in HR in IGF-1R depleted DU145 cells (13). However, impairment of ATM or HR induce only minor defects in repair of radiation-induced DSBs, apparent at ~24hr (31, 47), and unlikely to account for the early onset repair delay in IGF-1R-inhibited cells (Figure 4f).

In mammalian cells, rapid DSB repair is mediated principally via NHEJ (14). We employed three strategies to investigate whether IGF-1R inhibition influences the NHEJ pathway, assessing effects of AZ12253801 on expression of repair proteins, testing for epistasis between IGF-1R and DNA-PK, and performing repair reporter assays. Firstly, we found no evidence that AZ12253801 influenced levels of core NHEJ proteins in undamaged or irradiated cells, nor could we detect changes in expression of DSB sensing and HR components (Figure 4g). Repair protein function is not typically regulated at the level of

protein expression, but involves protein mobilization following induction of DNA damage (48). Therefore, we next sought evidence of involvement of the IGF axis in NHEJ by testing for functional interaction between IGF-1R and DNA-PK. M059J and M059K are human glioblastoma cell lines established from the same tumor, M059J being deficient in the catalytic subunit of DNA-dependent protein kinase (DNA-PKcs) and more radiosensitive than M059K (49). After confirming these differences in DNA-PKcs expression and intrinsic radiosensitivity (Figure 5a, b), we tested effects of IGF-1R inhibition. AZ12253801 enhanced radiosensitivity in the more radioresistant M059K cells, but not in DNAPKcs deficient M059J cells (Figure 5b). We noted that M059J cells expressed lower ATM levels than M059K (Figure 5a), potentially compromising interpretation of these results. However, this low level of ATM appeared to be functional, because ATM inhibition did radiosensitize both M059K and M059J cells (Supplementary Figure S5c). We next performed similar experiments in DU145 cells, testing for epistasis between IGF-1R and DNA-PK using DNA-PKcs inhibitor NU7441 (50). At 1μM, NU7441 blocked damage-induced DNA-PKcs autophosphorylation at Ser2056 without suppressing ATM activation as judged by Chk2 and KAP-1 phosphorylation (Figure 5c, Supplementary Figure S5d). We then used 1μM NU7441 in combination experiments in DU145 cells. As before (Figure 2f), AZ12253801 enhanced radiosensitivity of control-treated cells, but did not influence radiosensitivity in cells that were pre-treated with 1μM NU7441 (Figure 5d). Taken together, these data in glioblastoma and prostate cancer cells suggest that in the context of its effect on DSB repair, IGF-1R functions in the same pathway as DNA-PK.

Finally, we tested whether AZ12253801 induces functional impairment of repair, by measuring re-joining of DSB repair reporters integrated into the genomic DNA of HEK293 cells. We confirmed that these cells expressed IGF-1R, and that AZ12253801 could block IGF signalling (Figure 6a). At concentrations that we planned to use in repair assays, AZ12253801 induced accumulation in G2 phase of the cell cycle (Supplementary Figure S6, Table S2). In addition to integration of reporter constructs EJ5-GFP and DR-GFP that enable quantification of total NHEJ or HR respectively, these cells also express I-SceI as a fusion protein with flanking mutant estrogen receptor ligand binding domains (TAM), forming the TAM-I-SceITAM (TST) fusion for inducible I-SceI activation and DSB induction in response to 4-hydroxytamoxifen (4OHT; (51). We first tested effects of AZ12253801 on NHEJ, given that previous results (Figure 4d, 5b, d) implicated IGF-1R in regulation of this process. HEK293 EJ5-GFP-TST cells were treated with 4OHT and solvent or 30nM AZ12253801, and we also used 1μM NU7441 as a control for NHEJ inhibition. In solvent-treated controls we detected ~0.1% GFP positivity (Figure 6b), consistent with previously-published values of 0.2% GFP-positivity in 4OHT-treated mouse ES reporter cells and 0.05% in HEK293 cells (51). In HEK293 cells that were pre-treated with NU7441, GFP positivity was reduced to 30 ± 6% of control levels ($p<0.01$), supporting the ability of this assay to detect significant suppression of NHEJ. Rejoining of the NHEJ reporter was also suppressed by IGF-1R inhibition, to 40 ± 5% of control levels. This was significantly different from the solvent-control treated cells ($p<0.05$), but not from DNA-PK inhibited cells. These data suggest that AZ12253801 was capable of inhibiting DSB repair by NHEJ.

Having previously reported that *IGF1R* gene silencing suppresses repair by HR (13), we wanted to compare effects of IGF-1R inhibition on the two major DSB repair pathways in this HEK293 model. However, we were unable to detect GFP positivity in HEK293 DR-GFP-TST cells following 4OHT treatment (not shown). Therefore, as recommended (51), we used transient transfection of I-SceI to increase DSB yield. This approach generated detectable GFP positivity in control-treated cells, amounting to 5.7 ± 0.8% of EJ5-GFP (NHEJ reporter) transfectants and 1.6 ± 0.3% of DR-GFP (HR) transfectants (Figure 6c, d). NHEJ assays indicated that AZ12253801 induced dose-dependent inhibition of re-joining, with reduction to 69 ± 7% and 45 ± 5% in cells treated with 30nM and 60nM AZ12253801 respectively ($p<0.001$ for each comparison, Figure 6c). In comparison, DNA-PK inhibition suppressed re-joining to 26 ± 3 % of control levels ($p<0.001$); this effect was greater than that achieved by 30nM but not 60nM AZ12253801. Assays in HEK293 DR-GFP cells suggested that IGF-1R inhibition also suppressed HR, with reduction to ~65% of control values in cells treated with 30 or 60nM AZ12253801 ($p<0.05$; Figure 6d). These effects were comparable to the reduction in HR to 70% of control values we previously reported upon IGF-1R depletion (13), and also similar to effects of CDK1 inhibition (Figure 6d), reported to suppress HR by blocking CDK-induced phosphorylation of BRCA1 (52). These data suggest that IGF-1R inhibition influences DSB repair by both NHEJ and HR.

Discussion

Our data support previous findings that IGF-1R inhibition enhances sensitivity to ionizing radiation (2-4, 39). The use of low (sub-GI_{50}/SF_{50}) concentrations of IGF-1R inhibitor allowed us to distinguish effects of IGF-1R inhibition on DSB repair from other better-characterized phenotypes associated with IGF-1R. The results suggest that the ability of IGF-1R to influence DSB repair does not involve senescence induction and is largely independent of direct early effects on cell cycle distribution and apoptosis induction. This raised the question as to whether IGF-1R-inhibited cells die post-irradiation via alternative death mechanisms. IGF-1R inhibition was reported to induce mitotic catastrophe in a model of triple negative breast cancer (53), although this was in combination with the microtubule-stabilizing agent docetaxel that targets mitosis (54), and the IGF-1R inhibitor used for this study, BMS-754807, is reported to have activity against aurora kinases (55), which could contribute to this phenotype. Our data indicate that in both control and IGF-1R inhibited DU145 cells, abnormal mitoses were detectable 24hr after irradiation. Of relevance to this cell line model, we note that Rb loss was reported to be associated with radiation-induced genomic instability (56). At 5 days post-irradiation, IGF-1R inhibited DU145 cells manifest an increase in polyploidy and nuclear fragmentation compared with controls. These findings are consistent with the consequences of entry into mitosis with unrepaired or mis-repaired DNA damage (36, 37).

We now find direct evidence that IGF-1R inhibition induces a functional defect in DSB repair via the NHEJ pathway. Impairment of NHEJ (Figure 6) is consistent with the relatively large defect in DSB repair we documented previously in IGF-1R depleted cells (13), the early delay in resolution of radiation -induced γH2AX foci in IGF-1R inhibited DU145 cells (Figure 4d), and the demonstration of epistasis between IGF-1R and DNA-PK in prostate cancer and glioblastoma cells (Figure 5b, d). The finding of impaired end-joining

in IGF-1R inhibited cells is novel, and the molecular basis for this effect is unclear. At concentrations used here, AZ12253801 suppressed AKT activation (Figure 2c), and AKT has been linked with DSB repair, reported in different models either to promote NHEJ via DNA-PK activation, or to suppress HR and contribute to genome instability (57). IGF-1R has been reported to regulate both the expression of Ku80 (although we did not find evidence for this here; Figure 4g), and the ability of Ku proteins to bind double-stranded oligonucleotides (39). IGF-1R is also reported to be strongly associated with expression of Major Vault Protein (MVP), which is correlated with altered expression of Ku70/80 and apoptosis regulators, and with poor outcomes after radio-chemotherapy for cervical cancer (58, 59). Finally, we and others have described nuclear IGF-1R translocation (15, 60, 61), raising the prospect that nuclear IGF-1R could regulate the activity of repair proteins, as described for activation of DNA-PK by nuclear EGFR (62). However, we could not detect interaction between IGF-1R and DNA-PKcs (Supplementary Figure S5). Furthermore, radiosensitization was induced by AZ12253801 at concentrations below the GI_{50} (120nM) that we previously showed was required to block IGF-1R nuclear import (15), suggesting that IGF effects on NHEJ may be independent of nuclear IGF-1R.

Parallel assays testing effects of IGF-1R inhibition on DSB repair by HR are consistent with data we generated previously using *IGF1R* gene silencing. HR attenuation appears unrelated to the ability of the IGF axis to regulate cell cycle progression, given that we could detect delayed repair using low concentrations (30-60nM) of AZ12253801 that induced negligible early changes in cell cycle distribution (Table 2). The mitogenic effects of IGFs are principally mediated via cyclin D1 (63), but as noted elsewhere, Rb null cells such as DU145 do not show a proliferative response to cyclin D1 (64). It is increasingly recognized that cell cycle regulators including cyclin D1 and CDKs play important roles in HR (64, 65), and it is plausible that IGFs may influence the expression and/or activation of cell cycle regulators implicated in HR, even if such effectors do not promote cell cycle progression in the absence of Rb. Such a mechanism would not, however, explain the effect on NHEJ, and the demonstration of impaired repair by both NHEJ and HR raises the possibility that IGFs may regulate proteins or processes common to both pathways.

These findings have implications for the therapeutic efficacy and potential toxicity of IGF-1R inhibitors in the clinic. The involvement of IGF-1R in repair via NHEJ raises the prospect that IGF-1R inhibition could radiosensitize normal cells in G1, potentially enhancing dose-limiting toxicity to late-reacting tissues, although this possibility has not deterred development of DNA-PK inhibitors as radiosensitizers for clinical use (66). Because of uncertainty regarding toxicity, it may be preferable to assess novel radiosensitizers in the context of palliative rather than radical radiotherapy, and/or to perform a safety run-in phase involving escalation of the dose or duration of the biological agent with standard radiation protocols (67).

In conclusion, these data suggest that IGF-1R inhibition suppresses DSB repair by both NHEJ and HR, and induces biologically significant radio-sensitization of human and murine cells. Further investigation of the molecular basis for these effects will shed light on the role of IGF-1R, and may have implications for clinical use of IGF-1R inhibitors in combination with radiotherapy or DNA damaging cytotoxic drugs.

Materials and Methods

Cell lines and treatments

Prostate cancer cell lines DU145 and PC3 were obtained from Cancer Research UK Laboratories (Clare Hall Hertfordshire UK), and 22Rv1 and LNCaP-LN3 from Professor Sir Walter Bodmer (Department of Oncology, University of Oxford, UK). R− and R+ cells were from Dr Renato Baserga (Kimmel Cancer Center, Philadelphia, PA; (17). M059J and M059K glioblastoma cells (49) were from Dr Anne Kiltie (Department of Oncology, University of Oxford, UK). HEK-293 EJ5-GFP/TST and HEK293 DR-GFP/TST cells were obtained from Dr Wojciech Niedzwiedz (Department of Oncology, University of Oxford, UK) with permission from Professor Jeremy Stark (Beckman Research Institute of the City of Hope, California; (51). See Supplemental Methods for details of cell culture. AZ12253801 is an ATP-competitive IGF-1R inhibitor that was provided by AstraZeneca and previously described (15). DNA-PK inhibitor NU7441 was from Tocris Bioscience (Missouri, USA) and ATM inhibitor KU55933 and CDK1 inhibitor RO-3306 from Calbiochem (UK). Compounds were dissolved in dimethyl sulphoxide (DMSO) at 5mM (NU7441) or 10mM (AZ12253801, KU55933, RO-3306) and stored at −20°C. Gene silencing experiments used non-silencing Allstars siRNA and IGF-1R siRNA (Hs_IGF1R_1, Qiagen) as described (13). Cells were irradiated in a caesium-137 source (IBL 637 irradiator, CIS Bio International, France).

Western blotting, immunoprecipitation

Cells were lysed in IGF-1R lysis buffer (1%Triton-X-100; (13) or SDS lysis buffer in which 1% SDS replaced Triton-X-100. SDS lysates were sonicated on ice for 10sec continuously at maximum output (Sonopuls GM70, Bandelin, Germany). Lysates were analyzed by SDS polyacrylamide gel electrophoresis (SDS PAGE) and western blotting, using antibodies listed in Supplemental Methods. Immunoprecipitation was performed on precleared lysates prepared in IGF-1R lysis buffer as described (13) using antibodies to IGF-1R (#3027, Cell Signaling Technology, CST), IRS-1 (IRS-1 (#2382, CST) or irrelevant control (rabbit IgG, Sigma), for analysis by SDS PAGE and western blotting.

Assays for cell survival, apoptosis and senescence

Clonogenic assays were performed as in (13), using cells that were treated with solvent or drug(s), and after 4hr irradiated. This 4hr -pre-treatment was used to ensure that target inhibition was established prior to irradiation, based on time-course experiments (Figure 2d). For apoptosis assays, cells were seeded in black 96-well plates, and the following day treated and/or irradiated as above. Caspase 3/7 activity was quantified using Apo-ONE Homogeneous Caspase-3/7 Assays (Promega) according to the manufacturer's instructions. Fluorescence was measured at excitation and emission wavelengths of 499nm and 521nm respectively on a FLUOstar Optima fluorescence plate reader (BMG LabTech, Germany). After subtracting background fluorescence generated by medium without cells, fluorescence was expressed as % increase over solvent-treated control values [(treated- solvent)/ solvent × 100]. The Senescence Beta Galactosidase Staining Kit (Cell Signalling) was used according to the manufacturers recommendations. Briefly, cells were fixed with 20% formaldehyde, 2% glutaraldehyde, washed with PBS, and incubated overnight at 37°C with

the supplied staining solution containing X-gal. Visibly senescent primary renal cancer cells (provided by Mrs. Olga Perestenko, Department of Oncology, Oxford) were used as positive controls.

Flow cytometry

Cells were treated with solvent or AZ12253801, after 4hr irradiated, at intervals fixed in ice cold 80% ethanol with vortexing, and stored at −20°C. Cells were re-hydrated in PBS with 1% BSA (PBSB), centrifuged at 2,000 rpm for 5 min at room temperature, resuspended in PBS with 0.25% Triton X-100, and incubated on ice for 10mins. After centrifugation, cells were washed with PBSB, resuspended in PBS and incubated at room temperature for 30min with 10μg/ml propidium iodide (PI) and 100μg/ml RNAse prior to analysis. Cells were analyzed for mitotic index and ploidy as described (68) by staining with phospho-S10 histone H3 antibody (#ab5176 Abcam) and PI. Samples were analysed on a CyAn ADP Analyzer (Beckman-Coulter, UK) with FlowJo 7.6.5 software (www.flowjo.com).

Immunofluorescence

Cells were cultured on coverslips, irradiated and/or inhibitor treated, and fixed and stained as described (13) using primary antibodies to γH2AX (#2577, CST) phospho-S10 histone H3 (#ab5176 Abcam), β-tubulin (#T4026, Sigma), 53BP1 (#NB100-304, Novus Biologicals) and phospho-S2056 DNA-PKcs (#ab18192, Abcam), with Alexa Fluor 488 or 594 - conjugated anti-mouse and/or anti-rabbit secondary antibodies (Invitrogen Molecular Probes). Coverslips were mounted using Fluoromount G (Southern Biotech) with 2μg/ml 4′6-diamidino-2-phenylindole, dilactate (DAPI) and foci were imaged and counted on an Axioskop 2 Zeiss microscope (Carl Zeiss Ltd., UK).

DNA repair reporter assays

HEK293 reporter assays were performed as described (51), treating cells with solvent or small molecule inhibitors together with 3μM 4-hydroxytamoxifen (4OHT). After 24hr, the medium was replaced with fresh medium containing inhibitor without 4OHT. After a further 48hr cells were fixed in 4% paraformaldehyde, washed in PBS and resuspended in PBS for flow cytometry. Some assays used HEK293 cells seeded onto poly-L-lysine coated plates and transiently transfected the following day using Fugene HD (Promega) with pCMV-Sce and pDsRed2-Mito, or with eGFP cDNA or pDsRed2-Mito alone as controls for gating, as described (13). Four hours later, cells were treated with inhibitors, and after 72hr fixed for quantification of red and green fluorescence by flow cytometry.

Statistical analysis

Data were analysed using GraphPad Prism v5 (GraphPad Software Inc, USA), using t-tests to determine differences between two groups, one-way analysis of variance (ANOVA) for three or more groups, and two-way ANOVA for trends between response curves.

Supplementary Material

Refer to Web version on PubMed Central for supplementary material.

Acknowledgments

This work was supported by the NIHR Oxford Biomedical Research Centre, NIHR Research Capability Funding, Molecular and Cellular Medicine Board of the MRC, Cancer Research UK Clinical Research Fellowship to MMC, Prostate Cancer UK support to KL and TA, NIHR Research Capability Funding to KL, Breast Cancer Campaign for support to SG, and HEFCE Clinical Senior Lectureship to VMM. We are grateful to Elaine Kilgour and Elizabeth Anderson at AstraZeneca for providing AZ12253801, Walter Bodmer for LNCaP-LN3 cells, Renato Baserga for R+ and R-cells, Dr. Anne Kiltie for M059J and M059K cells, Jeremy Stark and Wojciech Niedzwiedz for HEK-293 EJ5-GFP/TST and HEK293 DR-GFP/TST cells, Olga Perestenko for primary renal cancer cells, and Peter McHugh and Tim Humphrey for comments on the manuscript.

References

1. Rochester MA, Riedemann J, Hellawell GO, Brewster SF, Macaulay VM. Silencing of the IGF1R gene enhances sensitivity to DNA-damaging agents in both PTEN wild-type and mutant human prostate cancer. Cancer gene therapy. 2005; 12(1):90–100. [PubMed: 15499378]
2. Riesterer O, Yang Q, Raju U, Torres M, Molkentine D, Patel N, et al. Combination of anti-IGF-1R antibody A12 and ionizing radiation in upper respiratory tract cancers. Int J Radiat Oncol Biol Phys. 2011; 79(4):1179–87. Epub 2010/12/07. [PubMed: 21129859]
3. Isebaert SF, Swinnen JV, McBride WH, Haustermans KM. Insulin-like growth factor-type 1 receptor inhibitor NVP-AEW541 enhances radiosensitivity of PTEN wild-type but not PTEN-deficient human prostate cancer cells. Int J Radiat Oncol Biol Phys. 2011; 81(1):239–47. Epub 2011/08/06. [PubMed: 21816290]
4. Ferte C, Loriot Y, Clemenson C, Commo F, Gombos A, Bibault JE, et al. IGF-1R targeting increases the antitumor effects of DNA damaging agents in SCLC model: an opportunity to increase the efficacy of standard therapy. Molecular cancer therapeutics. 2013 Epub 2013/05/04.
5. Molife LR, Fong PC, Paccagnella L, Reid AH, Shaw HM, Vidal L, et al. The insulin-like growth factor-I receptor inhibitor figitumumab (CP-751,871) in combination with docetaxel in patients with advanced solid tumours: results of a phase Ib dose-escalation, open-label study. Br J Cancer. 2010; 103(3):332–9. Epub 2010/07/16. [PubMed: 20628389]
6. Javle MM, Varadhachary GR, Fogelman DR, Shroff RT, Overman MJ, Ukegbu L, et al. Randomized phase II study of gemcitabine (G) plus anti-IGF-1R antibody MK-0646, G plus erlotinib (E) plus MK-0646 and G plus E for advanced pancreatic cancer. Journal of clinical oncology : official journal of the American Society of Clinical Oncology. 2011; 29(suppl) abstr 4026.
7. Yee D. Insulin-like growth factor receptor inhibitors: baby or the bathwater? J Natl Cancer Inst. 2012; 104(13):975–81. Epub 2012/07/05. [PubMed: 22761272]
8. Hellawell GO, Turner GD, Davies DR, Poulsom R, Brewster SF, Macaulay VM. Expression of the type 1 insulin-like growth factor receptor is up-regulated in primary prostate cancer and commonly persists in metastatic disease. Cancer Res. 2002; 62(10):2942–50. [PubMed: 12019176]
9. Grzmil M, Hemmerlein B, Thelen P, Schweyer S, Burfeind P. Blockade of the type I IGF receptor expression in human prostate cancer cells inhibits proliferation and invasion, up-regulates IGF binding protein-3, and suppresses MMP-2 expression. J Pathol. 2004; 202(1):50–9. Epub 2003/12/25. [PubMed: 14694521]
10. Krueckl SL, Sikes RA, Edlund NM, Bell RH, Hurtado-Coll A, Fazli L, et al. Increased insulin-like growth factor I receptor expression and signaling are components of androgen-independent progression in a lineage-derived prostate cancer progression model. Cancer Res. 2004; 64(23): 8620–9. Epub 2004/12/03. [PubMed: 15574769]
11. Liao Y, Abel U, Grobholz R, Hermani A, Trojan L, Angel P, et al. Up-regulation of insulin-like growth factor axis components in human primary prostate cancer correlates with tumor grade. Hum Pathol. 2005; 36(11):1186–96. Epub 2005/11/02. [PubMed: 16260272]
12. Sroka IC, McDaniel K, Nagle RB, Bowden GT. Differential localization of MT1-MMP in human prostate cancer tissue: role of IGF-1R in MT1-MMP expression. Prostate. 2008; 68(5):463–76. Epub 2008/01/16. [PubMed: 18196535]

13. Turney BW, Kerr M, Chitnis MM, Lodhia K, Wang Y, Riedemann J, et al. Depletion of the type 1 IGF receptor delays repair of radiation-induced DNA double strand breaks. Radiother Oncol. 2012; 103(3):402–9. Epub 2012/05/04. [PubMed: 22551565]
14. Jackson SP, Bartek J. The DNA-damage response in human biology and disease. Nature. 2009; 461(7267):1071–8. Epub 2009/10/23. [PubMed: 19847258]
15. Aleksic T, Chitnis MM, Perestenko OV, Gao S, Thomas PH, Turner GD, et al. Type 1 insulin-like growth factor receptor translocates to the nucleus of human tumor cells. Cancer Res. 2010; 70(16): 6412–9. Epub 2010/08/17. [PubMed: 20710042]
16. Shaw PH, Maughan TS, Clarke AR. Dual inhibition of epidermal growth factor and insulin-like 1 growth factor receptors reduce intestinal adenoma burden in the Apc(min/+) mouse. Br J Cancer. 2011; 105(5):649–57. Epub 2011/08/04. [PubMed: 21811251]
17. Sell C, Dumenil G, Deveaud C, Miura M, Coppola D, DeAngelis T, et al. Effect of a null mutation of the insulin-like growth factor I receptor gene on growth and transformation of mouse embryo fibroblasts. Mol Cell Biol. 1994; 14(6):3604–12. [PubMed: 8196606]
18. Tezuka M, Watanabe H, Nakamura S, Yu D, Aung W, Sasaki T, et al. Antiapoptotic activity is dispensable for insulin-like growth factor I receptor-mediated clonogenic radioresistance after gamma-irradiation. Clin Cancer Res. 2001; 7(10):3206–14. Epub 2001/10/12. [PubMed: 11595716]
19. Reiss K, Wang JY, Romano G, Furnari FB, Cavenee WK, Morrione A, et al. IGF-I receptor signaling in a prostatic cancer cell line with a PTEN mutation. Oncogene. 2000; 19(22):2687–94. [PubMed: 10851068]
20. McConkey DJ, Greene G, Pettaway CA. Apoptosis resistance increases with metastatic potential in cells of the human LNCaP prostate carcinoma line. Cancer Res. 1996; 56(24):5594–9. Epub 1996/12/15. [PubMed: 8971161]
21. Kurmasheva RT, Houghton PJ. IGF-I mediated survival pathways in normal and malignant cells. Biochimica et biophysica acta. 2006; 1766(1):1–22. Epub 2006/07/18. [PubMed: 16844299]
22. Dupont J, Holzenberger M. IGF type 1 receptor: a cell cycle progression factor that regulates aging. Cell Cycle. 2003; 2(4):270–2. Epub 2003/07/10. [PubMed: 12851467]
23. Bowen C, Birrer M, Gelmann EP. Retinoblastoma protein-mediated apoptosis after gamma-irradiation. J Biol Chem. 2002; 277(47):44969–79. Epub 2002/09/26. [PubMed: 12297496]
24. Kuemmerle JF, Zhou H, Bowers JG. IGF-I stimulates human intestinal smooth muscle cell growth by regulation of G1 phase cell cycle proteins. American journal of physiology Gastrointestinal and liver physiology. 2004; 286(3):G412–9. Epub 2003/11/01. [PubMed: 14592948]
25. Wu JD, Odman A, Higgins LM, Haugk K, Vessella R, Ludwig DL, et al. In vivo effects of the human type I insulin-like growth factor receptor antibody A12 on androgen-dependent and androgen-independent xenograft human prostate tumors. Clin Cancer Res. 2005; 11(8):3065–74. [PubMed: 15837762]
26. Flanigan SA, Pitts TM, Eckhardt SG, Tentler JJ, Tan AC, Thorburn A, et al. The insulin-like growth factor I receptor/insulin receptor tyrosine kinase inhibitor PQIP exhibits enhanced antitumor effects in combination with chemotherapy against colorectal cancer models. Clin Cancer Res. 2010; 16(22):5436–46. Epub 2010/10/15. [PubMed: 20943761]
27. Bielen A, Box G, Perryman L, Bjerke L, Popov S, Jamin Y, et al. Dependence of Wilms tumor cells on signaling through insulin-like growth factor 1 in an orthotopic xenograft model targetable by specific receptor inhibition. Proc Natl Acad Sci U S A. 2012; 109(20):E1267–76. Epub 2012/04/25. [PubMed: 22529373]
28. Hinz JM, Yamada NA, Salazar EP, Tebbs RS, Thompson LH. Influence of double-strand-break repair pathways on radiosensitivity throughout the cell cycle in CHO cells. DNA Repair (Amst). 2005; 4(7):782–92. Epub 2005/06/14. [PubMed: 15951249]
29. Shrivastav M, De Haro LP, Nickoloff JA. Regulation of DNA double-strand break repair pathway choice. Cell Res. 2008; 18(1):134–47. Epub 2007/12/25. [PubMed: 18157161]
30. Zhang R, Adams PD. Heterochromatin and its relationship to cell senescence and cancer therapy. Cell Cycle. 2007; 6(7):784–9. Epub 2007/03/23. [PubMed: 17377503]

31. Goodarzi AA, Noon AT, Deckbar D, Ziv Y, Shiloh Y, Lobrich M, et al. ATM signaling facilitates repair of DNA double-strand breaks associated with heterochromatin. Molecular cell. 2008; 31(2): 167–77. Epub 2008/07/29. [PubMed: 18657500]
32. Sprenger CC, Vail ME, Evans K, Simurdak J, Plymate SR. Over-expression of insulin-like growth factor binding protein-related protein-1(IGFBP-rP1/mac25) in the M12 prostate cancer cell line alters tumor growth by a delay in G1 and cyclin A associated apoptosis. Oncogene. 2002; 21(1): 140–7. Epub 2002/01/16. [PubMed: 11791184]
33. Scurr LL, Pupo GM, Becker TM, Lai K, Schrama D, Haferkamp S, et al. IGFBP7 is not required for B-RAF-induced melanocyte senescence. Cell. 2010; 141(4):717–27. Epub 2010/05/19. [PubMed: 20478260]
34. Ewald JA, Desotelle JA, Wilding G, Jarrard DF. Therapy-induced senescence in cancer. J Natl Cancer Inst. 2010; 102(20):1536–46. Epub 2010/09/23. [PubMed: 20858887]
35. Steiner MS, Zhang Y, Farooq F, Lerner J, Wang Y, Lu Y. Adenoviral vector containing wild-type p16 suppresses prostate cancer growth and prolongs survival by inducing cell senescence. Cancer gene therapy. 2000; 7(3):360–72. Epub 2000/04/15. [PubMed: 10766342]
36. Vakifahmetoglu H, Olsson M, Zhivotovsky B. Death through a tragedy: mitotic catastrophe. Cell death and differentiation. 2008; 15(7):1153–62. Epub 2008/04/12. [PubMed: 18404154]
37. Wouters, BG. Cell death after irradiation: how, when and why cells die. 4th Ed. Hodder Arnold; London UK: Great Britain: 2009. 2009
38. Trojanek J, Ho T, Del Valle L, Nowicki M, Wang JY, Lassak A, et al. Role of the insulin-like growth factor I/insulin receptor substrate 1 axis in Rad51 trafficking and DNA repair by homologous recombination. Mol Cell Biol. 2003; 23(21):7510–24. [PubMed: 14559999]
39. Cosaceanu D, Budiu RA, Carapancea M, Castro J, Lewensohn R, Dricu A. Ionizing radiation activates IGF-1R triggering a cytoprotective signaling by interfering with Ku-DNA binding and by modulating Ku86 expression via a p38 kinase-dependent mechanism. Oncogene. 2007; 26(17): 2423–34. Epub 2006/10/18. [PubMed: 17043647]
40. Lobrich M, Shibata A, Beucher A, Fisher A, Ensminger M, Goodarzi AA, et al. gammaH2AX foci analysis for monitoring DNA double-strand break repair: strengths, limitations and optimization. Cell Cycle. 2010; 9(4):662–9. Epub 2010/02/09. [PubMed: 20139725]
41. Ward IM, Chen J. Histone H2AX is phosphorylated in an ATR-dependent manner in response to replicational stress. J Biol Chem. 2001; 276(51):47759–62. Epub 2001/10/24. [PubMed: 11673449]
42. Solier S, Pommier Y. The apoptotic ring: a novel entity with phosphorylated histones H2AX and H2B and activated DNA damage response kinases. Cell Cycle. 2009; 8(12):1853–9. Epub 2009/05/19. [PubMed: 19448405]
43. Solier S, Pommier Y. MDC1 cleavage by caspase-3: a novel mechanism for inactivating the DNA damage response during apoptosis. Cancer Res. 2011; 71(3):906–13. Epub 2010/12/15. [PubMed: 21148072]
44. Wang B, Matsuoka S, Carpenter PB, Elledge SJ. 53BP1, a mediator of the DNA damage checkpoint. Science. 2002; 298(5597):1435–8. Epub 2002/10/05. [PubMed: 12364621]
45. Macaulay VM, Salisbury AJ, Bohula EA, Playford MP, Smorodinsky NI, Shiloh Y. Downregulation of the type 1 insulin-like growth factor receptor in mouse melanoma cells is associated with enhanced radiosensitivity and impaired activation of Atm kinase. Oncogene. 2001; 20(30):4029–40. [PubMed: 11494131]
46. Jeon JH, Kim SK, Kim HJ, Chang J, Ahn CM, Chang YS. Insulin-like growth factor-1 attenuates cisplatin-induced gammaH2AX formation and DNA double-strand breaks repair pathway in non-small cell lung cancer. Cancer letters. 2008; 272(2):232–41. Epub 2008/09/03. [PubMed: 18762365]
47. Rothkamm K, Kruger I, Thompson LH, Lobrich M. Pathways of DNA double-strand break repair during the mammalian cell cycle. Mol Cell Biol. 2003; 23(16):5706–15. Epub 2003/08/05. [PubMed: 12897142]
48. Polo SE, Jackson SP. Dynamics of DNA damage response proteins at DNA breaks: a focus on protein modifications. Genes & development. 2011; 25(5):409–33. Epub 2011/03/03. [PubMed: 21363960]

49. Allalunis-Turner MJ, Zia PK, Barron GM, Mirzayans R, Day RS 3rd. Radiation-induced DNA damage and repair in cells of a radiosensitive human malignant glioma cell line. Radiation research. 1995; 144(3):288–93. Epub 1995/12/01. [PubMed: 7494872]
50. Zhao Y, Thomas HD, Batey MA, Cowell IG, Richardson CJ, Griffin RJ, et al. Preclinical evaluation of a potent novel DNA-dependent protein kinase inhibitor NU7441. Cancer Res. 2006; 66(10):5354–62. Epub 2006/05/19. [PubMed: 16707462]
51. Bennardo N, Cheng A, Huang N, Stark JM. Alternative-NHEJ is a mechanistically distinct pathway of mammalian chromosome break repair. PLoS genetics. 2008; 4(6):e1000110. Epub 2008/06/28. [PubMed: 18584027]
52. Johnson N, Li YC, Walton ZE, Cheng KA, Li D, Rodig SJ, et al. Compromised CDK1 activity sensitizes BRCA-proficient cancers to PARP inhibition. Nat Med. 2011; 17(7):875–82. Epub 2011/06/28. [PubMed: 21706030]
53. Litzenburger BC, Creighton CJ, Tsimelzon A, Chan BT, Hilsenbeck SG, Wang T, et al. High IGF-IR activity in triple-negative breast cancer cell lines and tumorgrafts correlates with sensitivity to anti-IGF-IR therapy. Clin Cancer Res. 2011; 17(8):2314–27. Epub 2010/12/24. [PubMed: 21177763]
54. Fabbri F, Amadori D, Carloni S, Brigliadori G, Tesei A, Ulivi P, et al. Mitotic catastrophe and apoptosis induced by docetaxel in hormone-refractory prostate cancer cells. Journal of cellular physiology. 2008; 217(2):494–501. Epub 2008/07/11. [PubMed: 18615564]
55. Carboni JM, Wittman M, Yang Z, Lee F, Greer A, Hurlburt W, et al. BMS-754807, a small molecule inhibitor of insulin-like growth factor-1R/IR. Molecular cancer therapeutics. 2009; 8(12):3341–9. Epub 2009/12/10. [PubMed: 19996272]
56. Gonzalez-Vasconcellos I, Anastasov N, Sanli-Bonazzi B, Klymenko O, Atkinson MJ, Rosemann M. Rb1 haploinsufficiency promotes telomere attrition and radiation-induced genomic instability. Cancer Res. 2013; 73(14):4247–55. Epub 2013/05/21. [PubMed: 23687339]
57. Xu N, Lao Y, Zhang Y, Gillespie DA. Akt: a double-edged sword in cell proliferation and genome stability. Journal of oncology. 2012; 2012:951724. Epub 2012/04/07. [PubMed: 22481935]
58. Lloret M, Lara PC, Bordon E, Fontes F, Rey A, Pinar B, et al. Major vault protein may affect nonhomologous end-joining repair and apoptosis through Ku70/80 and bax downregulation in cervical carcinoma tumors. Int J Radiat Oncol Biol Phys. 2009; 73(4):976–9. Epub 2009/03/03. [PubMed: 19251084]
59. Valenciano A, Henriquez-Hernandez LA, Moreno M, Lloret M, Lara PC. Role of IGF-1 receptor in radiation response. Translational oncology. 2012; 5(1):1–9. Epub 2012/02/22. [PubMed: 22348170]
60. Sehat B, Tofigh A, Lin Y, Trocme E, Liljedahl U, Lagergren J, et al. SUMOylation mediates the nuclear translocation and signaling of the IGF-1 receptor. Sci Signal. 2010; 3(108):ra10. Epub 2010/02/11. [PubMed: 20145208]
61. Sarfstein R, Pasmanik-Chor M, Yeheskel A, Edry L, Shomron N, Warman N, et al. Insulin-like growth factor-I receptor (IGF-IR) translocates to nucleus and autoregulates IGF-IR gene expression in breast cancer cells. J Biol Chem. 2012; 287(4):2766–76. Epub 2011/12/01. [PubMed: 22128190]
62. Dittmann K, Mayer C, Fehrenbacher B, Schaller M, Raju U, Milas L, et al. Radiation-induced epidermal growth factor receptor nuclear import is linked to activation of DNA-dependent protein kinase. J Biol Chem. 2005; 280(35):31182–9. Epub 2005/07/08. [PubMed: 16000298]
63. Kornmann M, Arber N, Korc M. Inhibition of basal and mitogen-stimulated pancreatic cancer cell growth by cyclin D1 antisense is associated with loss of tumorigenicity and potentiation of cytotoxicity to cisplatinum. The Journal of clinical investigation. 1998; 101(2):344–52. Epub 1998/02/07. [PubMed: 9435306]
64. Jirawatnotai S, Hu Y, Michowski W, Elias JE, Becks L, Bienvenu F, et al. A function for cyclin D1 in DNA repair uncovered by protein interactome analyses in human cancers. Nature. 2011; 474(7350):230–4. Epub 2011/06/10. [PubMed: 21654808]
65. Yata K, Esashi F. Dual role of CDKs in DNA repair: to be, or not to be. DNA Repair (Amst). 2009; 8(1):6–18. Epub 2008/10/04. [PubMed: 18832049]

66. Bolderson E, Richard DJ, Zhou BB, Khanna KK. Recent advances in cancer therapy targeting proteins involved in DNA double-strand break repair. Clin Cancer Res. 2009; 15(20):6314–20. Epub 2009/10/08. [PubMed: 19808869]

67. Harrington KJ, Billingham LJ, Brunner TB, Burnet NG, Chan CS, Hoskin P, et al. Guidelines for preclinical and early phase clinical assessment of novel radiosensitisers. Br J Cancer. 2011; 105(5):628–39. Epub 2011/07/21. [PubMed: 21772330]

68. Roberts DJ, Spellman RA, Sanok K, Chen H, Chan M, Yurt P, et al. Interlaboratory assessment of mitotic index by flow cytometry confirms superior reproducibility relative to microscopic scoring. Environ Mol Mutagen. 2012; 53(4):297–303. Epub 2012/02/22. [PubMed: 22351437]

69. Sramkoski RM, Pretlow TG 2nd, Giaconia JM, Pretlow TP, Schwartz S, Sy MS, et al. A new human prostate carcinoma cell line, 22Rv1. In vitro cellular & developmental biology Animal. 1999; 35(7):403–9. Epub 1999/08/26. [PubMed: 10462204]

70. Fraser M, Zhao H, Luoto KR, Lundin C, Coackley C, Chan N, et al. PTEN deletion in prostate cancer cells does not associate with loss of RAD51 function: implications for radiotherapy and chemotherapy. Clin Cancer Res. 2012; 18(4):1015–27. Epub 2011/11/25. [PubMed: 22114138]

71. Lehmann BD, McCubrey JA, Jefferson HS, Paine MS, Chappell WH, Terrian DM. A dominant role for p53-dependent cellular senescence in radiosensitization of human prostate cancer cells. Cell Cycle. 2007; 6(5):595–605. Epub 2007/03/14. [PubMed: 17351335]

72. Scott SL, Earle JD, Gumerlock PH. Functional p53 increases prostate cancer cell survival after exposure to fractionated doses of ionizing radiation. Cancer Res. 2003; 63(21):7190–6. Epub 2003/11/13. [PubMed: 14612513]

73. Mujoo K, Watanabe M, Khokhar AR, Siddik ZH. Increased sensitivity of a metastatic model of prostate cancer to a novel tetravalent platinum analog. Prostate. 2005; 62(1):91–100. Epub 2004/09/25. [PubMed: 15389812]

Europe PMC Funders Author Manuscripts

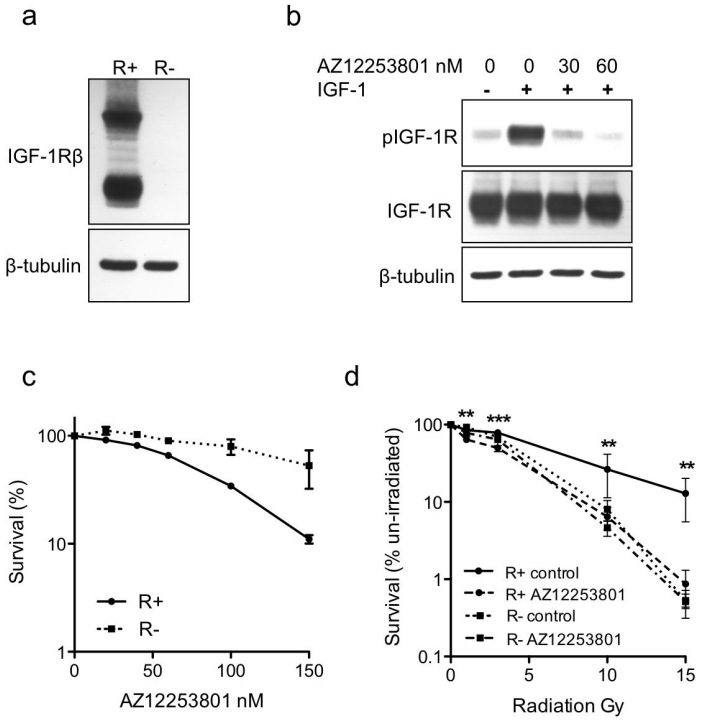

Figure 1. AZ12253801 inhibits IGF-1R activation and enhances radiosensitivity of IGF-1R-overexpressing R+ cells but not IGF-1R null R− cells

a) R+ and R− lysates analyzed by western blot for IGF-1R. **b)** Serum-starved R+ cells were pre-treated with solvent or AZ12253801 for 4hr and in the final 15min with 50nM IGF-1. **c)** Cells were treated with solvent or AZ12253801. After 11-12 days, visible colonies were stained and counted. Graph shows cell survival expressed as mean ± SEM % survival in solvent-treated controls from three independent experiments, each with triplicate dishes. The survival curves were significantly different (p=0.0005 by 2-way ANOVA). **d)** Cells were treated with solvent or 60nM AZ12253801 for 4hrs prior to irradiation, and clonogenic survival was measured as in c). Points represent mean ± SEM for triplicate values in three separate experiments. AZ12253801 inhibited survival of R+ (**p<0.01, ***p< 0.001 by one way ANOVA) but not R− cells.

Europe PMC Funders Author Manuscripts

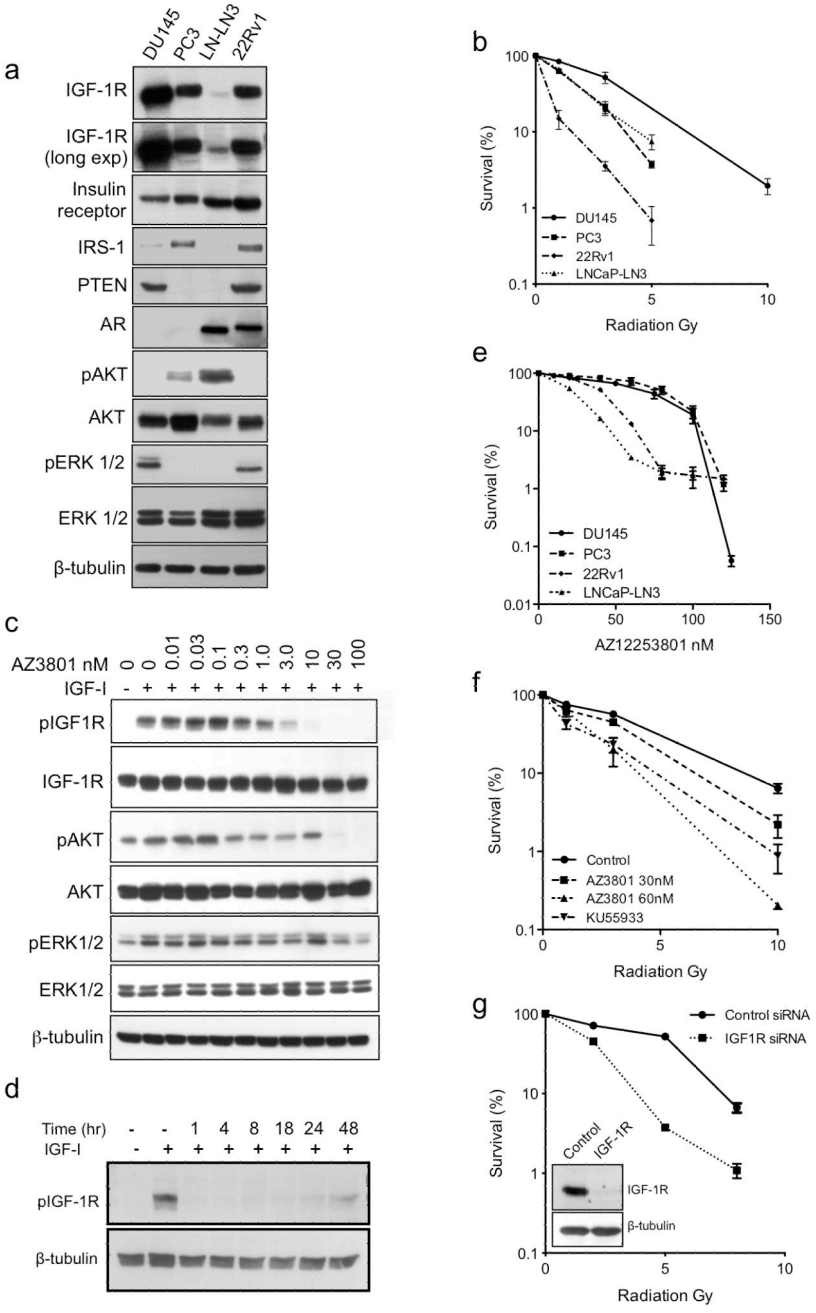

Figure 2. Human prostate cancer cells are radiosensitized by IGF-1R inhibition

a) Whole cell lysates were prepared from prostate cancer cells for western blotting. **b)** Intrinsic radiosensitivity of prostate cancer cell lines. Cells were seeded at 3000 cells/10cm dish and the following day were irradiated. Graph shows % survival in unirradiated controls; points represent mean ± SEM survival from three independent experiments. **c, d)** Serum-starved DU145 cells were treated with c) solvent or 0.01-100nM AZ12253801 for 4hr, or d) 30nM AZ12253801 for 1-48hr, and in the final 15 min with 50nM IGF-1. **e)** Prostate cancer cells were treated with solvent or AZ12253801. Pooled data from three independent assays

for each cell line were curve-fitted using GraphPad Prism v5 to interpolate SF_{50} values, shown in Table 1. **f)** DU145 cells were treated with solvent (Control), 30 or 60nM AZ12253801 or 10μM ATM inhibitor KU55933 for 4hr prior to irradiation. Graph shows cell survival from three independent assays expressed as % survival in unirradiated cells. Compared with control-treated cells, cell survival was reduced by pre-treatment with AZ12253801 at 30nM following 10 Gy ($p<0.05$ by one way ANOVA), and at 60nM following 3 ($p<0.001$) and 10 Gy ($p<0.05$). KU55933 radiosensitized to 1, 3 and 10 Gy ($p<0.001$ for each comparison); these effects were not significantly different from radiosensitization induced by 30nM AZ12253801 at 10Gy, or 60nM AZ12253801 at 1-10 Gy. **g)** DU145 cells were transfected with 50nM Allstars non-silencing control siRNA or IGF-1R siRNA, the following day reseeded for clonogenic assay, and 4hr later irradiated. The survival of IGF-1R depleted cells was significantly reduced compared with controls ($p<0.001$ at 2, 5 and 8 Gy). Inset: western blot to confirm IGF-1R depletion.

Europe PMC Funders Author Manuscripts

Europe PMC Funders Author Manuscripts

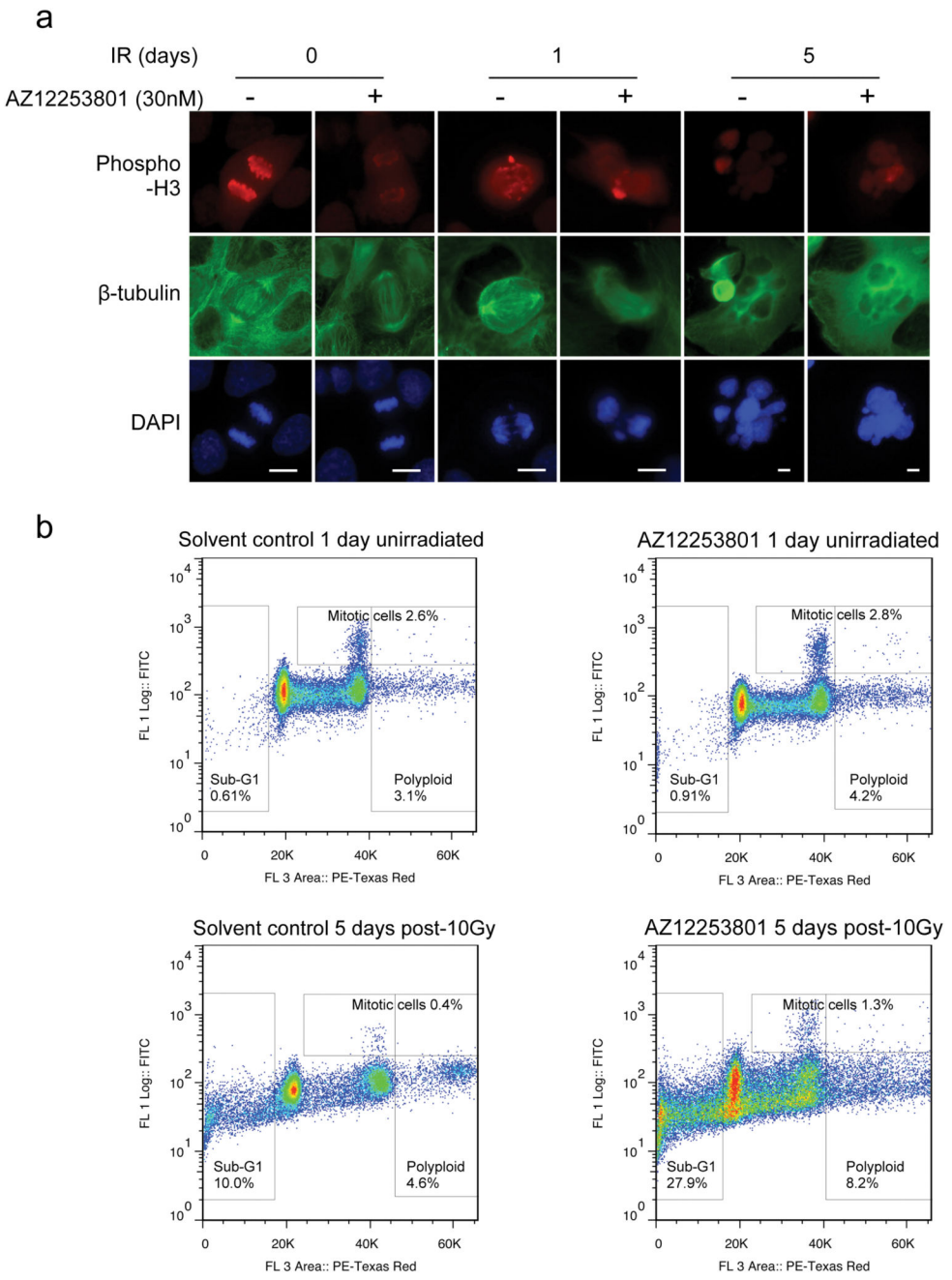

Figure 3. IGF-1R inhibition enhances radiation-induced polyploidy and late nuclear fragmentation

a) DU145 cells were treated with solvent or 30nM AZ12253801 for 4hr and some cells were irradiated (10Gy). Irradiated cells were fixed after 1 or 5 days, unirradiated controls were fixed after 1 day, and cells were stained for phospho-histone H3, β-tubulin and DNA (DAPI). Original magnification x40. Similar but less frequent morphological changes were seen after 3Gy (not shown). **b)** Cells were treated and irradiated as a), fixed, stained with phosphohistone H3 and PI, and 50,000 cells per condition were analyzed by flow cytometry.

Scatter plots show phospho-histone H3 (Y-axis) plotted against PI (DNA content, X-axis), gated to quantify mitotic (phospho-histone H3 positive), polyploid (>4N DNA content) and fragmented cells (sub-G1 DNA content).

Europe PMC Funders Author Manuscripts

Europe PMC Funders Author Manuscripts

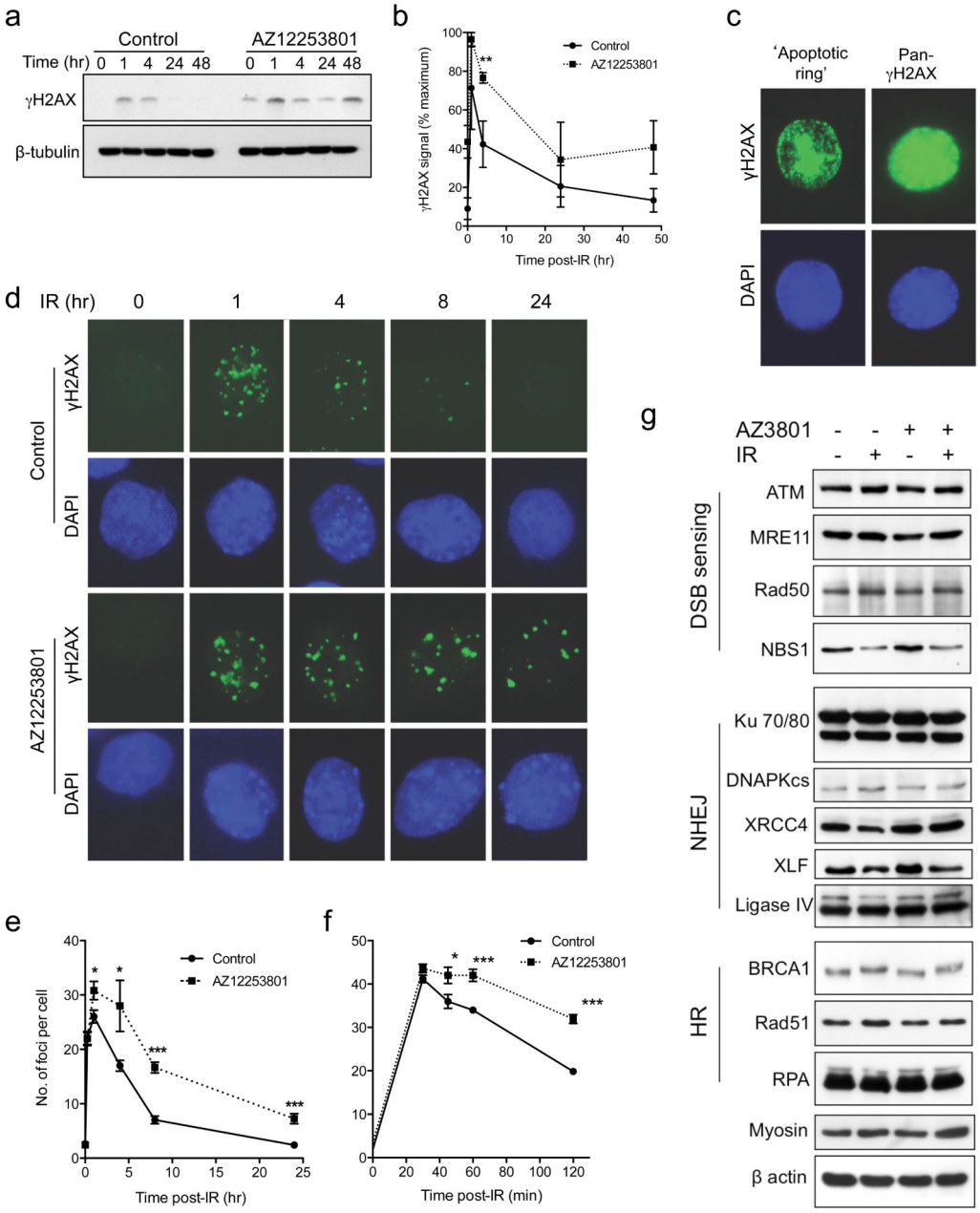

Figure 4. IGF-1R inhibition delays resolution of irradiation-induced DSBs

a) DU145 cells were incubated for 4hr with 30nM AZ12253801, irradiated (3Gy) and lysed at time-points post-irradiation for analysis by western blot. **b)** Graph shows γH2AX signal intensity with time, corrected for loading and expressed as % maximal signal in control cells. Points represent mean ± SEM of three independent experiments. At 4hr there was a significant excess of γH2AX signal in IGF-1R-inhibited cells (**p<0.01). **c, d)** DU145 cells were treated with AZ12253801 and irradiated as in a), and at intervals fixed and stained for S139 γH2AX and DAPI (DNA), showing representative images of c) cells with intense,

non-focal γH2AX signal that may reflect apoptosis; such cells were excluded from subsequent analysis; d) cells pre-irradiation (0 hr), and 1 - 24hr post-irradiation. Original magnification x40. **e, f)** Cells pre-treated with 30nM AZ12253801 and irradiated as above were analysed by counting foci in ≥60 cells per condition. Graphs show mean focus count per cell ± SEM for three independent experiments, over time-course of: e) 0-48 hr, f) 0-2 hr. IGF-1R-inhibited cells contained significantly more γH2AX foci than controls from 1 – 24 hr post-irradiation (*$p<0.05$, ***$p<0.001$ by t-test). **g)** DU145 cells were treated with 60nM AZ12253801 for 4hrs, irradiated (5Gy), and 4hr later lysed for western blotting for proteins involved in DSB sensing, NHEJ and HR. Myosin Iib (230 kDa) was used as loading control for proteins >200kDa.

Europe PMC Funders Author Manuscripts

Europe PMC Funders Author Manuscripts

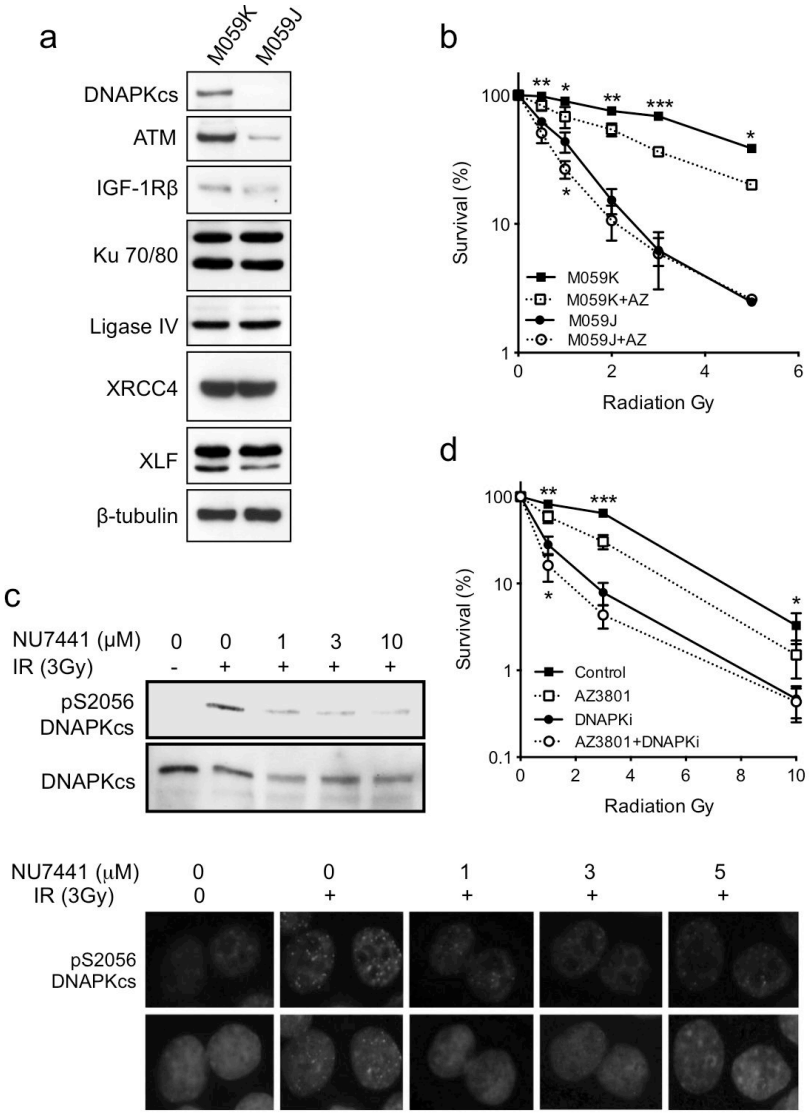

Figure 5. IGF-1R inhibition is epistatic with DNAPKcs deficiency or inhibition

a) M059J and MO59K cells were lysed in SDS lysis buffer for analysis by western blot to determine levels of ATM and core NHEJ proteins. **b)** M059J and M059K cells were treated with 30nM AZ12253801 for 4hr and irradiated. Cell survival was expressed as % survival in unirradiated controls. Points represent mean ± SEM for triplicate values in three separate experiments, each with triplicate data points. AZ12253801 enhanced radiosensitivity of M059K cells but not M059J cells (*p<0.05, **p<0.01, ***p<0.001). **c)** DU145 cells were treated with DNA-PK inhibitor NU7441 for 4hrs, irradiated (3 Gy) and 1hr post-irradiation: upper, lysed for western blot to assess DNA-PKcs S2056 autophosphorylation; lower, fixed and stained for phospho-S2056 DNAPKcs, showing representative radiation-induced pS2056 DNAPKcs foci (green) merged with DAPI (blue). **d)** DU145 cells were treated with solvent (Control), 30nM AZ12253801 (AZ3801), 1μM NU7441 (DNA-PKi) or a combination of AZ12253801 and NU7441 for 4hrs prior to irradiation. Cell survival was

expressed as % survival in unirradiated controls. Points represent mean ± SEM for triplicate values in three separate experiments. AZ12253801 enhanced radiosensitivity of control-treated DU145 cells (*p<0.05, **p<0.01, ***p<0.001). Aside from minor sensitization at 1 Gy (*p<0.05), AZ12253801 did not further enhance the radiosensitivity of DNA-PK-inhibited cells.

Europe PMC Funders Author Manuscripts

Europe PMC Funders Author Manuscripts

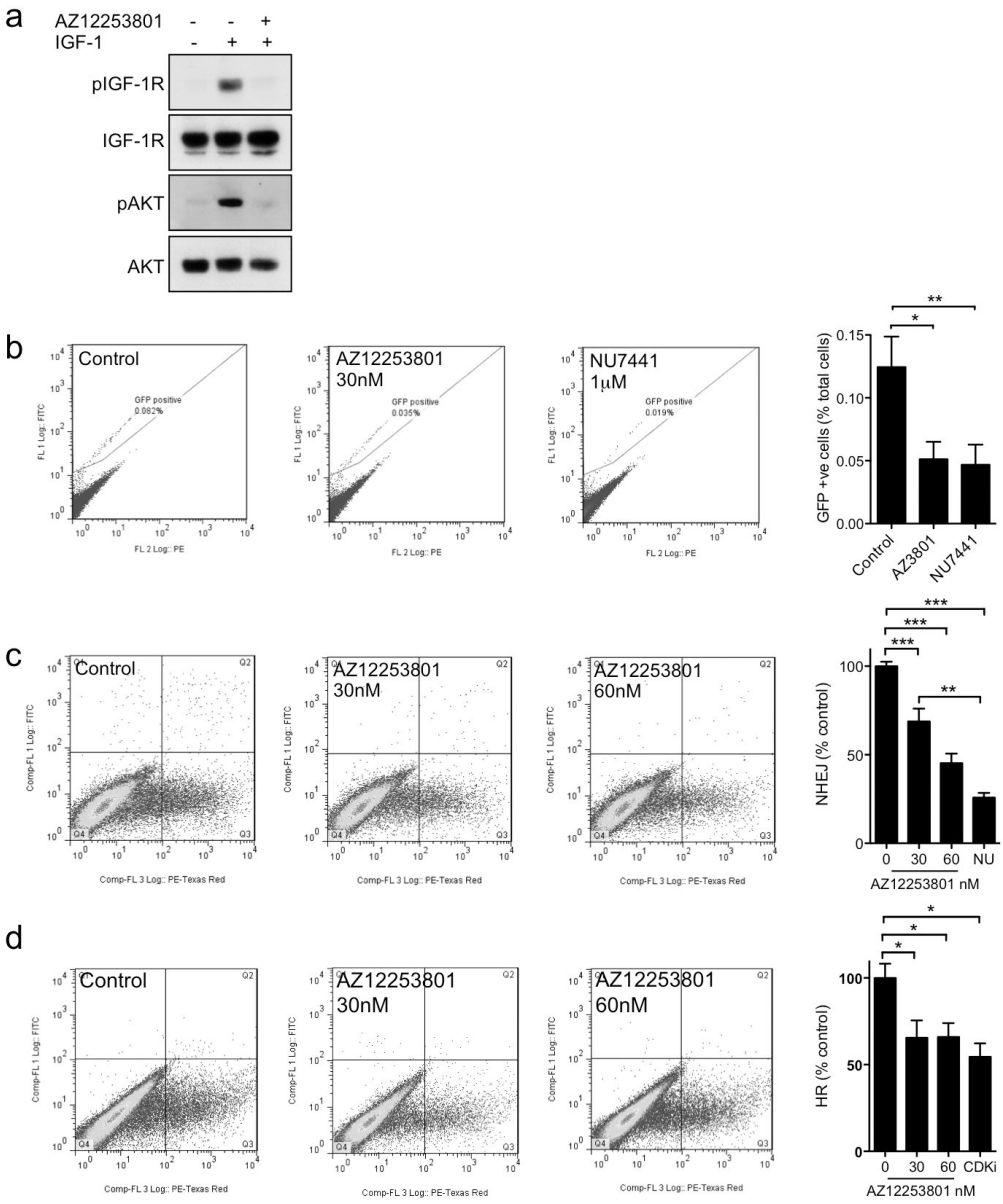

Figure 6. IGF-1R inhibition suppresses DSB repair by both NHEJ and HR

a) Serum-starved EJ5-GFP-TST HEK293 cells were treated with 30nM AZ12253801 for 4hr and with 50nM IGF-1 for the final 15min prior to lysis. **b)** EJ5-GFP-TST HEK293 cells were treated with solvent, 30nM AZ12253801 or 1μM NU7441, together with 3μM 4OHT. After 24hr, 4OHT-containing medium was removed and replaced with fresh medium containing inhibitors, and 72hr after initial 4OHT treatment the cells were analysed by flow cytometry. Representative analyses are shown of solvent-treated controls and cells treated with AZ12253801 or NU7441. Graph shows mean ± SEM GFP positivity in 3 independent

assays each with triplicate samples (*p<0.05, **p<0.01 by one way ANOVA). **c)** EJ5-GFP TST HEK293 cells or **d)** pDR-GFP-TST HEK293 cells were transfected with pDsRed2-Mito and pCMV-SceI, and 4hr later treated with solvent, 30 or 60nM AZ12253801, 1μM NU7441 (NU) or 1μM RO-3306 (CDK inhibitor, CDKi). After 72hr, red and green fluorescence were quantified by flow cytometry. GFP positivity was calculated as green cells (upper right quadrant) as a percent of total transfected cells (red; upper right plus lower right quadrants), and excluded GFP positive, pDsRed2-Mito negative cells (upper left quadrant). Graphs show mean ± SEM GFP positivity expressed as % control, in 3 independent assays each with triplicate samples (*p<0.05, **p<0.01, ***p<0.001 by one way ANOVA).

Europe PMC Funders Author Manuscripts

Europe PMC Funders Author Manuscripts

Table 1
Response of prostate cancer cell lines to IGF-1R inhibition

Genotypes from COSMIC (Catalogue of Somatic Mutations in Cancer; http://cancer.sanger.ac.uk) and (19, 69-73). WT, wild-type; MT, mutant; AR, androgen receptor; IRS-1, insulin-receptor substrate-1. Effect of AZ12253801 (AZ3801) on sensitivity to 3 Gy ionizing radiation, calculated as ratio of % survival of controls vs AZ12253801-treated cells.

	Genotype				AZ3801 SF_{50} (nM)	Sensitization to 3 Gy IR
Cell Line	**PTEN**	**p53**	**AR**	**Other**		
DU145	WT (+/−)	MT	Absent	Rb null	60	2.8
PC3	Null (−/−)	Null (−/−)	Absent		80	3.8
22Rv1	WT (+/+)	WT (+/−)	Present		30	2.4
LNCaP-LN3	MT (+/−)	WT (+/+)	Present	IRS-1 null	20	1.3

Europe PMC Funders Author Manuscripts

Table 2

Effects of IGF-1R inhibition on sub-G1, mitotic and polyploid (>4N) fractions after irradiation

DU145 cells were treated as legend to Figure 3 with solvent (Control) or 30nM AZ12253801 (AZ3801) for 4hr, irradiated (3 or 10 Gy) and collected at intervals for analysis of mitotic index (phospho-histone H3 positivity) and DNA content.

		3 Gy			10 Gy		
	Day	Sub-G1 (%)	Mitotic (%)	>4N (%)	Sub-G1 (%)	Mitotic (%)	>4N (%)
Control	1	1.0	3.5	5.2	1.8	8.7	3.4
	2	1.6	4.9	5.4	5.2	6.4	5.0
	3	2.7	3.6	2.9	8.3	5.0	6.5
	5	12.1	0.5	4.4	10.0	0.4	4.6
AZ3801	1	1.0	4.1	2.9	1.7	7.2	1.8
	2	2.0	3.8	3.9	7.9	6.1	4.4
	3	4.7	4.9	5.4	12.1	4.4	6.4
	5	12.6	0.9	4.1	27.9	1.3	8.2